Charge Transport in Chemically Doped 2D Graphene

Aurélien Lherbier,[1,3] X. Blase,[2] Yann-Michel Niquet,[3] François Triozon,[4] and Stephan Roche[5]

[1]*Laboratoire des Technologies de la Microélectronique (LTM), UMR 5129 CNRS, 17 Rue des Martyrs 38054 Grenoble, France*
[2]*Institut Néel, CNRS and Université Joseph Fourier, B.P. 166, 38042 Grenoble cedex 09, France*
[3]*CEA, Institute for Nanosciences and Cryogenics (INAC), SP2M/L_Sim, 17 rue des Martyrs, 38054 Grenoble Cedex 9, France*
[4]*CEA, LETI-Minatec, 17 rue des Martyrs, 38054 Grenoble Cedex 9, France*
[5]*CEA, Institute for Nanosciences and Cryogenics (INAC), SPSMS/GT 17 rue des Martyrs, 38054 Grenoble Cedex 9, France*

(Received 26 March 2008; published 18 July 2008)

We report on a numerical study of electronic transport in chemically doped 2D graphene materials. By using *ab initio* calculations, a self-consistent scattering potential is derived for boron and nitrogen substitutions, and a fully quantum-mechanical Kubo-Greenwood approach is used to evaluate the resulting charge mobilities and conductivities of systems with impurity concentration ranging within [0.5, 4.0]%. Even for a doping concentration as large as 4.0%, the conduction is marginally affected by quantum interference effects, preserving therefore remarkable transport properties, even down to the zero temperature limit. As a result of the chemical doping, electron-hole mobilities and conductivities are shown to become asymmetric with respect to the Dirac point.

DOI: 10.1103/PhysRevLett.101.036808 PACS numbers: 73.63.−b, 72.15.Rn, 81.05.Uw

The recent fabrication of a single graphene layer exfoliated from graphite material has triggered tantalizing enthusiasm for new discoveries [1]. Indeed, the 2D graphene sheet exhibits a unique electronic band structure with a linear dispersion relation close to the charge neutrality point (or Dirac point). The chiral nature of charge excitations in 2D graphene has been shown to result in unconventional quantum transport features, such as unusual quantum Hall effects [2], or anomalously weak localization phenomena at low temperature [2,3]. Charge mobilities in the range $1 - 20 \times 10^3$ cm^2 V^{-1} s^{-1} were reported in graphene samples with various levels of disorder [4]. In the low density limit, the corresponding conductivity values were found to vary within $[2, 15]e^2/h$. A comprehensive semiclassical theory of charge transport, based on a self-consistent calculation of scattering potentials and Bloch-Boltzmann equation, has been proposed recently [5]. However, such an approach is expected to break down in the low carrier density limit, complicating the understanding of the conductivity minimum observed experimentally, or the further investigation of quantum interference phenomena at low temperatures. Indeed, the precise contribution of quantum interferences in disordered 2D graphene remains fiercely debated [3], with no experimental evidence of strong Anderson localization, in contrast to the prediction of conventional 2D scaling theory of localization in disordered systems [6].

The rise of 2D graphene science is also accelerated by the technological expectations that have emerged in the field of carbon-based nanoelectronics. In addition to the exfoliation procedure, an alternative approach to fabricate ultrathin graphene layers-based materials has been proposed for large scale integration [7]. Notwithstanding, if undoped 2D graphene shows unprecedented capability to convey huge current densities [8], reported field-effect transistors exhibit relatively poor performances (on/off current ratio hardly reaching 1 order of magnitude) [1], despite the possibility to design quasi-1D graphene nanoribbons with enlarged confinement-induced energy gaps [9].

Chemical doping provides a natural way to enhance the performances of 2D graphene-based devices. Remarkable chemical sensor properties of graphene have already been reported [10], whereas a novel field-effect graphene device based on an electrochemical switch principle has been demonstrated [11]. Efficient p-type (n-type) doping of graphene can be achieved, respectively, through the incorporation of boron (nitrogen) atoms in substitution within the carbon matrix. Using chemical vapor deposition (CVD), boron-doped graphite thin films with concentrations up to $\sim$10% could be fabricated [12]. The presence of impurity states and the strong disruption of sp^2 long-range order were further clearly evidenced by STM and Raman characterizations [13]. Some first study of the effect of boron on graphene ribbon edges has already been performed [14]. However to date, 2D mesoscopic transport in intentionally chemically doped (and disordered) graphene remains unexplored from both theoretical and experimental perspectives.

In this Letter, we report on the first extensive numerical study of charge transport in boron (and nitrogen) doped 2D graphene sheets, using the Kubo-Greenwood transport formalism that allows to explore all transport regimes, including localization effects beyond the semiclassical approximation. In the low concentration limit ($\sim$0.1%), the conduction remains ballistic up to $\sim$500 nm (reaching computational capability). For larger doping concentration ($\geq$0.5%), a clear diffusive regime is observed, allowing the extraction of the corresponding elastic mean free paths, semiclassical conductivities and charge mobilities as a function of charge carrier energy and doping density. Interestingly, the chemical disorder is found to induce some electron-hole asymmetry of all transport features.

Some onset of weak localization is also observed for sufficiently large doping concentrations ($\geq 2.0\%$), although the contribution of quantum interferences remains too weak to produce a transition to a strongly localized regime within the micron scale.

We describe the chemically doped graphene systems using an efficient tight-binding (TB) Hamiltonian within the orthogonal first nearest neighbor $\pi - \pi$ model (hopping term $\gamma = -2.7$ eV). This model accurately reproduces the band structure of the pristine graphene plane around the Dirac point [15]. To model the effect of boron (B) [or nitrogen (N)] doping on the π electrons, extensive *ab initio* calculations were performed within the density functional theory [16]. We used large 14×14 graphene supercells with carbon atoms randomly substituted by B(N) atoms for various doping concentrations. After structural relaxation, we analyzed the self-consistent change in the p_z orbital onsite and hopping terms around the dopant [18]. The effect of charging through the gate was also mimicked by adding electrons or holes [21] to the graphene sheet and rerunning the self-consistent cycles to update the charge density and related Hartree plus exchange and correlation potential. The introduction of the impurity potential in the TB Hamiltonian is carried out by renormalizing the p_z orbital onsite energies of the around the dopant atom j, following the self-consistent *ab initio* potential profile $V(r - r_j)$ [19,20]. A realistic disordered potential profile can thus be generated by random substitutions of C atoms by B or N atoms. It is characterized by the doping concentration (C_d), which allows us to tune the disorder strength. We found that for low concentrations $C_d \sim 0.1\%$, the transport remains quasiballistic over several hundreds of nanometers. In the following, we focus on various concentrations $C_d = [0.5\%, 1.0\%, 2.0\%, 4.0\%]$, for which a clear diffusive regime establishes, allowing for the exploration of charge mobility and conductivity scaling properties. We first discuss the densities of states (DOS) of ideal and chemically disordered 2D graphene sheets. As shown in Fig. 1(a) (dashed lines), the ideal DOS (spin included) is characterized by two main features: i.e., a linear dependence in energy around the Dirac point and two Van Hove singularities around $\pm\gamma$. When dopants are introduced, the Fermi level is shifted away from the Dirac point and the van Hove singularities are steadily broadened with doping density. Besides, as evidenced by the local density of states around a single impurity [Figs. 1(b) and 1(c)], the effect of boron and nitrogen impurities is symmetrical with respect to the Dirac point, so we focus on boron (p-type) doping from hereon.

The energy and time dependence of the diffusion coefficient $D(E, t)$ are computed within the Kubo-Greenwood formalism, which allows the extraction of the elastic mean free path $\ell_e(E)$, semiclassical conductivity $\sigma_{sc}(E)$ and charge carrier mobility $\mu(E)$, as discussed in [22,23]. The different transport regimes are identified through the time dependence of D. The ballistic regime corresponds to a linear behavior of D, whereas the diffusive regime develops once D saturates to a maximum value $D_{max}(E)$. The mean free path $\ell_e(E)$ and charge mobility $\mu(E)$ can be thus computed from $D_{max}(E)$. More precisely, $\ell_e(E) = D_{max}(E)/2v(E)$ with $v(E)$ the mean velocity at energy E, while $\sigma_{sc}(E) = 1/4(e^2\rho(E)D_{max}(E))$ [with $\rho(E)$ the DOS and e the elementary charge], and $\mu(E) = \sigma_{sc}(E)/n(E)e$ with $n(E)$ the carrier density with respect to the Dirac point. Finally, a decay of $D(t)$ evidences the contribution of quantum interferences that may eventually lead to a strong Anderson-type localization regime. In Fig. 2(a), the time dependence of $D(E, t)$ at the energy corresponding to the Dirac point [represented by closed symbols in Fig. 2(b)] are shown for different values of C_d. The diffusion coefficient D has been renormalized with respect to D_{max} to allow an easier comparison between the different

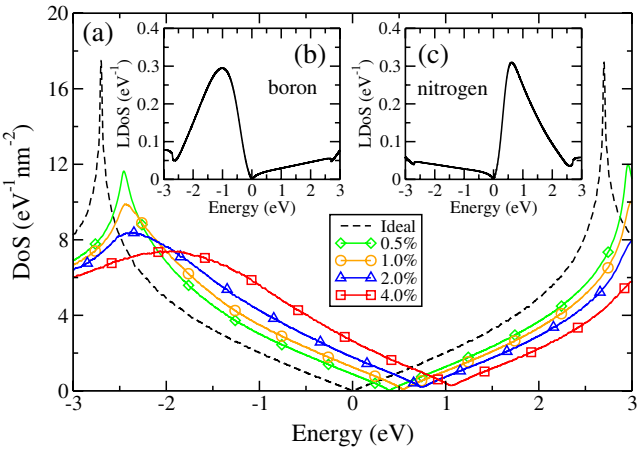

FIG. 1 (color online). (a) Density of states of an ideal (dashed line) and boron-doped graphene sheets for several values of C_d. The zero of the energy has been set to the Fermi levels. (b),(c) local density of states on a boron (b) and nitrogen (c) impurity.

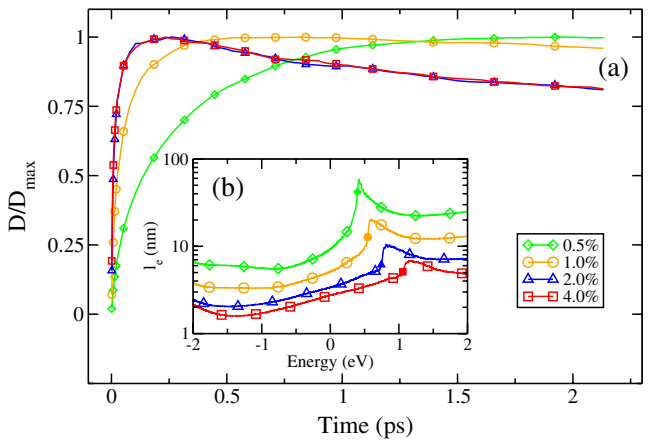

FIG. 2 (color online). (a) Normalized time-dependent diffusion coefficient for a charge energy corresponding to the Dirac point, and several C_d. The closed symbols locate the position of the Dirac point (b) elastic mean free path as a function of energy for $C_d = 0.5\%$, 1.0%, 2.0%, and 4.0%.

curves. For $C_d = 0.5\%$, a ballistic regime is first observed at short time scales, followed by a long transition regime before the saturation of D. The diffusive (saturation) regime is more quickly reached when C_d is increased, and for $C_d \geq 2.0\%$ the diffusive regime directly establishes after a very short time. The corresponding energy-dependent mean free paths ℓ_e are shown in a log scale in Fig. 2(b), for $C_d = 0.5\%$, 1.0%, 2.0%, and 4.0%, and range within $\sim[5, 60]$ nm close to the Dirac point. One first notes that for low doping density ℓ_e decays as $\sim 1/C_d$, in good agreement with the Fermi golden rule. More interesting, is the observed asymmetry between hole and electron mean free paths. This asymmetry follows from the nature of the chemical scattering potential which differently impacts electrons and holes, resulting in ℓ_e which can change by a factor of 2 for the same energy shift with respect to the Dirac point. The mobility μ is plotted as a function of Fermi energy and doping concentration in Fig. 3(a). It has been computed both at zero (dotted lines) and room temperature (full lines), taking the Fermi-Dirac broadening into account. Here the chemical (doping) disorder is assumed to dominate over electron-phonon scattering [9]. The effect of the thermal broadening on the mobility clearly turns out to be very limited, in agreement with the reported weak temperature dependence of experimental measurements [4]. As pointed out in Ref. [4], although the conductivity $\sigma_{sc}(E)$ remains always finite, the definition of the mobility yields a divergence at the Dirac point since the carrier density $n(E)$ tends to zero. μ is nonetheless meaningful for finite (and experimentally relevant) carrier densities. Depending on C_d, our computed mobilities are found to range within $\simeq [7 \times 10^2, 4 \times 10^3]$ cm^2 V^{-1} s^{-1} for $n(E) = 10^{12}$ cm^{-2} electrons/holes. In Fig. 3(b), the asymmetry between the electron (μ^e) and hole (μ^h) mobilities is shown for $C_d = 0.5\%$ and a larger carrier density range. Similarly to the mean free path, μ^e and μ^h are found to differ by a factor ~ 2 in the low doping limit.

In Fig. 4(a), the conductivity $\sigma_{sc}(E)$ is shown as a function of charge energy, for both the zero (dotted lines) and room temperature (full lines) regime. At zero temperature, σ_{sc} depends on the doping concentration, and drops to its minimal value at the Dirac point. Typically, for doping concentration ranging from 0.5% to 4.0%, one gets $\sim 2 - 3e^2/h$. For $C_d \leq 0.5\%$, this drop becomes more peaked and thus can be significantly smoothen by temperature broadening, resulting in a higher minimum value at room temperature ($\sim 7 - 8e^2/h$ for $C_d = 0.5\%$). The horizontal dashed line in Fig. 4(a) pinpoints the value of $2G_0/\pi = 4e^2/h\pi$ (with $G_0 = 2e^2/h$ the quantum conductance) that has been analytically derived within the self-consistent Born approximation (SCBA) [24]. It is seen that this SCBA value stands as a semiclassical minimum which is, however, not reached even in situations of large doping. The long-range nature of the scattering potential was initially proposed to be at the origin of some universal minimum conductivity value at the Dirac point, related to the absence of localization effects [3,24]. In a set of recent experiments [4], significant sample to sample fluctuations have been reported with conductivity varying within $[2, 10]e^2/h$, whereas the dominating scattering mechanism was attributed to charged impurities trapped in the oxide layer.

Beyond semiclassical effects, the issue of *anomalous localization in disordered graphene* has been fiercely debated [3]. It was theoretically argued that if short range disorder should trigger usual localization effects, backscattering, and quantum interferences close to the Dirac point could be strongly damped, or even suppressed, in presence of a long-range scattering potential [3]. Here, the scattering potential due to substitutional chemical impurities presents

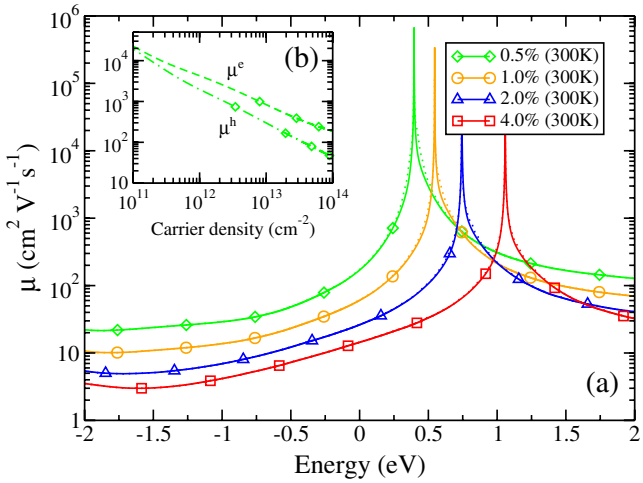

FIG. 3 (color online). (a) Charge mobility at room temperature as a function of Fermi energy and C_d. Dotted lines correspond to the zero temperature limit. (b) Charge mobilities for electrons (dashed lines) and holes (dashed-dotted lines) as a function of the carrier density and for $C_d = 0.5\%$.

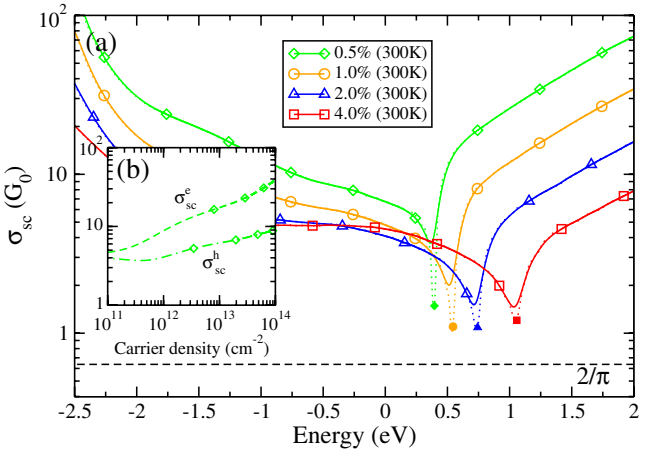

FIG. 4 (color online). (a) Semiclassical conductivity at room temperature as a function of energy and C_d. Dotted lines correspond to the zero temperature limit. (b) Semiclassical conductivities for electrons (dashed lines) and holes (dashed-dotted lines) as a function of the carrier density and for $C_d = 0.5\%$.

both short range (since there is a substantial onsite impurity energy renormalization) as well as some long-range features. For sufficiently high concentration, such as $C_d \geq 2.0\%$, D clearly decays after the maximum diffusivity [see Fig. 2(a)], indicating the onset of quantum interference effects. The observed asymmetry in the elastic mean free paths and charge mobilities also applies to the contribution of quantum interferences, and holes are found to be more sensitive to localization phenomena for boron doping, in contrast to the case of nitrogen doping which impacts more strongly on electron transport (not shown here). Finally, by using the conventional 2D localization scaling theory [6], an estimation of the localization length at the Dirac point gives $\xi \sim 4\ \mu$m ($\xi \sim 200$ nm) for $C_d = 0.5\%$ ($C_d = 4\%$) showing the robustness of the diffusive regime up to the micron scale in the low doping limit. Enhanced impurity concentrations (5%–10%) might induce stronger localization effects, but such severely chemically modified graphene materials might also suffer from marked atomic distortions, whose description is beyond the scope of the present study.

In conclusion, the physics of charge transport in chemically doped disordered 2D graphene has been theoretically investigated using a full quantum-mechanical transport approach and *ab initio* derived diffusion potentials. The resulting electron and hole transport features were found to be asymmetric with respect to the Dirac point, with minimum conductivities ranging within $\sim[2, 8]e^2/h$ depending on the doping level and carrier density, whereas the contribution of quantum interferences was found marginal even for disorder as large as $C_d \sim 4.0\%$. This suggests that chemical doping is a viable way to tailor the graphene properties without impeding its good conducting behavior.

Financial support from FP7-ICT GRAND project and CARNOT Institute-Leti are acknowledged.

[1] K. S. Novoselov *et al.*, Science **306**, 666 (2004).
[2] A. K. Geim and K. S. Novoselov, Nat. Mater. **6**, 183 (2007); B. Oezyilmaz *et al.*, Appl. Phys. Lett. **91**, 192107 (2007); B. Oezyilmaz *et al.*, Phys. Rev. Lett. **99**, 166804 (2007); Z. Jiang, Y. Zhang, H. L. Stormer, and Ph. Kim, Phys. Rev. Lett. **99**, 106802 (2007); K. S. Novoselov *et al.*, Science **315**, 1379 (2007); Y. Zhang *et al.*, Phys. Rev. Lett. **96**, 136806 (2006); Y. Zhang *et al.*, Nature (London) **438**, 201 (2005).
[3] E. McCann *et al.*, Phys. Rev. Lett. **97**, 146805 (2006); H. Suzuura and T. Ando, J. Phys. Soc. Jpn. **75**, 024703 (2006); V. I. Fal'ko *et al.*, Solid State Commun. **143**, 33 (2007); F. W. Tikhonenko *et al.*, Phys. Rev. Lett. **100**, 056802 (2008).
[4] C. O. Girit and A. Zettl, Appl. Phys. Lett. **91**, 193512 (2007); Y.-W. Tan *et al.*, Phys. Rev. Lett. **99**, 246803 (2007); S. Cho and M. S. Fuhrer, Phys. Rev. B **77**, 081402 (2008); J. H. Chen *et al.*, Nature Nanotechnology **3**, 206 (2008); J. H. Chen *et al.*, Nature Phys. **4**, 377 (2008).
[5] S. Adam, E. H. Hwang, V. M. Galitski, and S. Das Sarma, Proc. Natl. Acad. Sci. U.S.A. **104**, 18 392 (2007); E. H. Hwang, S. Adam, and S. Das Sarma, Phys. Rev. Lett. **98**, 186806 (2007).
[6] P. A. Lee and T. V. Ramakrishnan, Rev. Mod. Phys. **57**, 287 (1985).
[7] C. Berger *et al.*, Science **312**, 1191 (2006).
[8] J. Moser, A. Barreiro, and A. Bachtold, Appl. Phys. Lett. **91**, 163513 (2007).
[9] M. C. Lemme *et al.*, IEEE Electron Device Lett. **28**, 282 (2007); M. Y. Han, B. Oezyilmaz, Y. Zhang, and Ph. Kim, Phys. Rev. Lett. **98**, 206805 (2007); Z. Chen *et al.*, Physica (Amsterdam) **40E**, 228 (2007); S. V. Morozov *et al.*, Phys. Rev. Lett. **100**, 016602 (2008); X. Li *et al.*, Science **319**, 1229 (2008).
[10] F. Schedin *et al.*, Nat. Mater. **6**, 652 (2007); E. H. Hwang, S. Adam, and S. Das Sarma, Phys. Rev. B **76**, 195421 (2007); T. O. Wehling *et al.*, Nano Lett. **8**, 173 (2008); R. Ruoff, Nature Nanotechnology **3**, 10 (2008).
[11] T. J. Echtermeyer, M. C. Lemme, M. Braus, B. N. Szafranek, A. K. Geim, and H. Kurz, (to be published).
[12] B. M. Way *et al.*, Phys. Rev. B **46**, 1697 (1992); C. T. Hach *et al.*, Carbon **37**, 221 (1999).
[13] M. Endo *et al.*, J. Appl. Phys. **90**, 5670 (2001).
[14] T. B. Martins, R. H. Miwa, A. J. R. da Silva, and A. Fazzio, Phys. Rev. Lett. **98**, 196803 (2007).
[15] J. C. Charlier, X. Blase, and S. Roche, Rev. Mod. Phys. **79**, 677 (2007).
[16] Our calculations are based on the SIESTA package [17] in the local density approximation, with a double-ζ basis for each atom.
[17] D. Sánchez-Portal, P. Ordejon, E. Artacho, and J. M. Soler, Int. J. Quantum Chem. **65**, 453 (1997).
[18] The reliability of our approach has been tested by comparing the tight-binding and *ab initio* transmission (see Refs. [19,20]) in the case of doped nanotubes.
[19] H. J. Choi, J. Ihm, S. G. Louie, and M. L. Cohen, Phys. Rev. Lett. **84**, 2917 (2000).
[20] Ch. Adessi, S. Roche, and X. Blase, Phys. Rev. B **73**, 125414 (2006).
[21] The injected charges are compensated by an opposite sign background uniform jellium, so that the unit cells remain neutral. Such a technique is now very standard in the study of charged impurities using supercell approaches.
[22] F. Triozon *et al.*, Phys. Rev. B **69**, 121410 (2004); A. Lherbier, B. Biel, Y.-M. Niquet, and S. Roche, Phys. Rev. Lett. **100**, 036803 (2008); S. Roche and R. Saito, Phys. Rev. Lett. **87**, 246803 (2001); F. Triozon *et al.*, Phys. Rev. B **65**, 220202 (2002).
[23] Periodic boundary conditions are applied, and large enough planes are considered to avoid any spurious effects on the disorder potential. Convergence is achieved for $L_x = 300$ nm by $L_y = 245$ nm planes which enclose up to 2.8 millions of carbon atoms. Averages over tens of different disorder configurations are performed for the calculation of transport coefficients.
[24] T. Ando, J. Phys. Soc. Jpn. **75**, 074716 (2006); K. Ziegler, Phys. Rev. Lett. **97**, 266802 (2006); K. Nomura and A. H. MacDonald, Phys. Rev. Lett. **96**, 256602 (2006); J. Cserti, Phys. Rev. B **75**, 033405 (2007).